Evidence of geomagnetic effect on extensive air showers

P. Bernardini [1] [2] , C. Bleve[1] [2], A. D'Amone[1] [2], I. De Mitri[1] [2], G. Mancarella[1] [2], G. Marsella[1] [2], L. Perrone[1] [2], and A. Surdo[2]

[1]Dipartimento di Matematica e Fisica "E. De Giorgi", Università del Salento, Italy

[2]Istituto Nazionale di Fisica Nucleare, Sezione di Lecce, Italy,

1. Introduction

The path of charged primary cosmic rays (CR) is deflected by magnetic fields. The galactic magnetic field randomizes the CR directions. The geomagnetic field (GeoMF) restrains low-rigidity CR's from reaching the terrestrial atmosphere and causes that the CR flux is lower from East than from West. The GeoMF acts also on the charged particles of the extensive air showers (EAS) during their travel in the atmosphere [1]. If the trigger efficiency of an array is sensitive to the shower lateral extension, the GeoMF can change the acquisition rate as a function of zenith and azimuth angles. This effect has been studied analyzing the data collected by the ARGO-YBJ experiment. The results of this analysis have been presented in many conferences [2] and they are are fully presented in the paper [3].

ARGO-YBJ array [4] is located in the YangBaJing (YBJ) village (Tibet, P.R. of China) at 4300 m above sea level ($90°31'50''E$, $30°06'38''N$). The full-coverage active area used for trigger purpose is 74×78 m^2. The collected EAS have a typical energy in the range $1 - 200$ TeV, well beyond the rigidity cutoff. Therefore the effect of the GeoMF on the primary trajectory is negligible.

In the ARGO-YBJ reference system the azimuth angle (ϕ) of EAS is defined with respect to the detector axes in the counterclockwise direction ($\phi = 0°$ for showers aligned with the x-axis and moving towards the positive direction). Thus in the ARGO-YBJ reference system the azimuth angle of showers going towards the magnetic North is $\phi_B = 71.89° \pm 0.02°$. The geomagnetic field at YBJ is $B = 49.7$ μT with zenith angle $\theta_B = 46.4°$.

2. Toy model and simulation

The trajectory of the EAS charged particles is deflected by the GeoMF in the plane perpendicular to $\vec{B}$ (hereafter named bending plane). Assuming small angular deviations and relativistic particles, the value (d) of the West-East shift on the shower front is expected to be

$$d = \frac{qL^2}{2p}\ B\ sin\,\xi, \tag{1}$$

where q is the charge, p the particle momentum, L the path length and ξ the angle between $\vec{B}$ and $\vec{p}$. This shift of the charged particle path in the bending plane is the main effect of the GeoMF action. The model should take into account that each particle in the shower has different values of p, θ, ϕ and h. In short a MonteCarlo simulation is necessary. Anyway Eq. (1) indicates an enlargement of the shower footprint. This implies a decrease of the particle density near the shower core, which is then balanced by an increase at larger distances [5]. As a consequence a very small, direction dependent, reduction in the ARGO-YBJ trigger efficiency can be envisaged for showers with the core lying inside the carpet.

Beams of primary protons have been simulated in order to study the magnetic effect and to disentagle it from detector effects. Hereafter the angular coordinates (θ, ϕ) are those of the shower axis, not those of the single particles. The CORSIKA code has been used to reproduce the showers and a GEANT3-based code to simulate the detector response. Simulated and real data have been studied with the same analysis chain.

By means of a simulation without GeoMF the detector acceptance has been studied. It introduces an azimuthal modulation with maximum at 90° and periodicity 180°. The modulation amplitude (g_{2A}) has been estimated from the real data. The GeoMF effect on the reconstruction of the EAS direction is negligible, whereas it is significant on the trigger efficiency. Neglecting the detector effect, the rate (λ) is dependent on $sin^2\,\xi$ according to

$$\lambda = \lambda_{max}\left(1 - \eta\ sin^2\,\xi\right). \tag{2}$$

The term η depends linearly also on B^2, thus the rate reduction is proportional to $B^2 sin^2\,\xi$ and is due to the GeoMF stretching of the EAS footprint. In other words the reduction of the charge

density close to the core actually reduces the trigger efficiency when the core is on the array.

Neglecting the detector effect, the CR-beam simulation suggests that the trigger efficiency depends on the coupling between GeoMF and EAS charged particles. From Eq. (2) we conclude that the number of events (N_θ) in an angular $\Delta\theta \times \Delta\phi$ window depends on ξ as

$$N_\theta = N_{\theta,max}\ (1 - \eta\, sin^2\,\xi), \tag{3}$$

where $N_{\theta,max}$ is the number of events expected without magnetic field and η is the previous parameter, fixed by B value, detector features and trigger conditions. A two-harmonics function is got by the calculation of $sin^2\,\xi$:

$$N_\theta = N_{\theta,0}\,\{1 + g_1 cos\,(\phi - \phi_1) + g_2 cos\,[2\,(\phi - \phi_2)]\}\,, \tag{4}$$

where

$$\phi_1 = \phi_2 = \phi_B, \tag{5}$$

$$N_{\theta,0} = N_{\theta,max}\,(1 - \eta\, A_0)\,, \tag{6}$$

$$g_1 = \frac{\eta\, sin 2\theta_B}{2(1 - \eta\, A_0)}\, sin\, 2\theta, \tag{7}$$

$$g_2 = \frac{\eta\, sin^2\theta_B}{2(1 - \eta\, A_0)}\, sin^2\theta, \tag{8}$$

$$A_0 = sin^2\theta_B + \left(1 - \frac{3}{2} sin^2\theta_B\right) sin^2\theta. \tag{9}$$

3. Data analysis

The data set has been collected in $6.77 \times 10^5\ s$, the array has been carefully time-calibrated with the characteristic plane method [6]. Two analysis cuts have been applied: shower core reconstructed inside a square of $40 \times 40\ m^2$ at the center of the carpet, zenith angle lower than 60°. The first cut has been chosen in order to make more evident the trigger efficiency decrease (the effect is very different for showers with the core far from the detector). These cuts guarantee also a more reliable reconstruction of the shower direction.

The dependence of the number of events on $sin^2\,\xi$ according to formula (3) is the first possible check. In Fig. 1 each scattered point represents the number of events in an angular window plotted versus $sin^2\,\xi$. The θ value is fixed for each group of points meanwhile ϕ is running. The $sin^2\,\xi$ range depends on θ, it is maximum for $\theta = 45°$ and minimum for θ close to 0°. The scattered points are fitted by function (3), which is then confirmed to give a good description of the data. The η values from the fit are displayed in Fig. 2 with respect to θ.

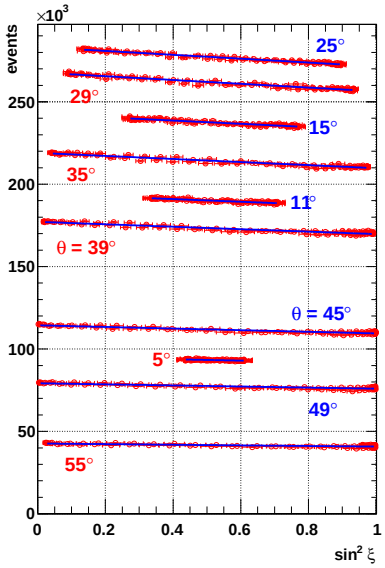

Figure 1. Real data: scatter plot of the number of events in $\Delta\theta \times \Delta\phi = 2° \times 5°$ windows versus $sin^2\,\xi$ for different values of θ. Fits with function (3) are superimposed.

By integrating all showers in the range $\theta < 60°$ the azimuthal distribution is shown in Fig. 3. It is well fitted by the double harmonic function (4). The phase of the first harmonic ($\phi_1 = 72.75° \pm 0.29°$) is compatible with the GeoMF azimuth ($\phi_B = 71.89°$) as expected if the origin of the modulation is geomagnetic. This is not the case of the second harmonic phase (ϕ_2) with a value very close to what expected for the detector effect.

The azimuthal distribution has been studied also in θ-ranges of 2° in order to check the dependence of g_1 and g_2 on θ. The result for g_1 is shown in Fig. 3 and the fit with function (7) confirms that η is constant with respect to θ. We stress that g_1 depends only on the GeoMF effect. The fractional variation of the term $(1 - \eta A_0)$ is less

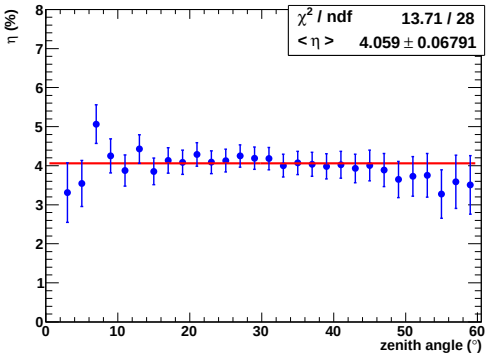

Figure 2. Real data: the parameter η versus θ.

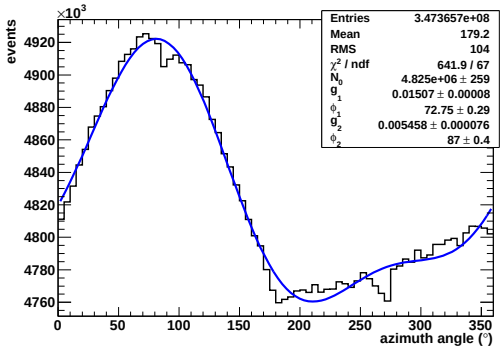

Figure 3. Real data: azimuthal distribution and fit with function (4).

than 0.7% for $\theta < 60°$. Then g_1 is mainly proportional to $sin\,2\theta$. Meanwhile the first harmonic is in full agreement with the GeoMF model, this is not the case for the second harmonic. The tension can be solved simply taking into account that the detector effect observed in the simulation without magnetic field operates on the second harmonic. Therefore the second harmonic can be split in two parts: one ($2B$) is due to the GeoMF, the other one ($2A$) to the detector acceptance. Three data sets have been selected on the basis of the zenith angle in order to disentagle these two effects. The ϕ-distributions of the subsamples (α for $\theta < 20°$, β for $20° < \theta < 40°$ and γ for $40° < \theta < 60°$) can be fitted with a single function:

$$N_i = N_{i,0}\left\{1 + \frac{\eta\ sin2\theta_B}{2(1-\eta A_0)}\langle sin\,2\theta\rangle_i\ cos\,(\phi-\phi_1) + \frac{\eta\ sin^2\theta_B}{2(1-\eta A_0)}\langle sin^2\theta\rangle_i\ cos\,[2\,(\phi-\phi_1)] + g^i_{2A}\ cos\,[2\,(\phi-\phi_{2A})]\right\}, \qquad (10)$$

where the coefficients of the magnetic component are deduced from Eq.s (7) and (8), the phase ϕ_1 is used for first and magnetic second harmonic and $i = \alpha, \beta, \gamma$ indicates the subsamples. The fit results are reported in Table 1, the phase ϕ_1 and the GeoMF azimuth ϕ_B are in agreement, the η value is very close to the previous estimate. The coefficients g^i_{2A} increase with θ and ϕ_{2A} is close to 90° as expected for a detector effect.

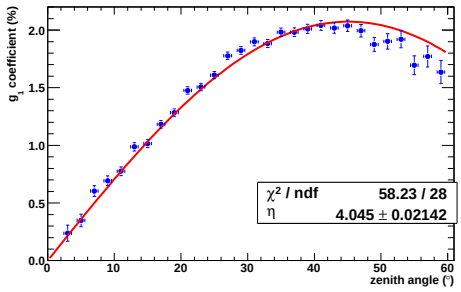

Figure 4. Real data: coefficient g_1 versus zenith angle. The fit with function (7) is superimposed.

η (%)	4.060 ± 0.019
ϕ_1 (°)	72.22 ± 0.28
g^{α}_{2A} (%)	0.124 ± 0.013
g^{β}_{2A} (%)	0.271 ± 0.011
g^{γ}_{2A} (%)	1.076 ± 0.019
ϕ_{2A} (°)	96.30 ± 0.47

Table 1
Results of the fit with function (10) of three azimuthal distributions.

We conclude that the azimuthal modulation depends on a mix of magnetic and detector effects. The GeoMF origin of the rate reduction is leading with respect to the detector effect in the zenith range $20° - 40°$ where $g_{2A} << g_1$. Taking also into account that g_{2A} increases with θ the rising η values for $\theta > 50°$ of the rate-vs-$sin^2\xi$ analysis (Fig. 2) are explained.

4. Conclusions

The effect of the geomagnetic Lorentz force on EAS charged particles has been observed. The shower extension is enlarged depending on the arrival direction with respect to the GeoMF and the different charge density reduces the trigger efficiency for EAS with the core on the detector. The GeoMF origin and the features of the trigger efficiency decrease are fully understood.

The azimuthal distribution is well described by two harmonics, the first one of the order of 1.5%, the second one of the order of 0.5%. The first harmonic is due to the GeoMF, the second one is the sum of magnetic and detector effects. The measured geomagnetic phase is fully compatible with the expected value. More details on this analysis are available in [3].

REFERENCES

1. G. Cocconi, Phys. Rev. 93 (1954) 646.
2. P. Bernardini *et al.*, Proc. of 32nd Internat. Cosmic Ray Conf. (Beijing, 2011) 0755 (also arXiv:1110.0670); P. Bernardini *et al.*, Journ. of Physics: Conf. Series 409 (2013) 012229.
3. B. Bartoli *et al.* (ARGO-YBJ Collaboration), Phys. Rev. D 89 (2014) 05205.
4. G. Aielli *et al.* (ARGO-YBJ Collaboration), Nucl. Instr. & Meth. A 661 (2012) S50.
5. A.A. Ivanov *et al.*, JETP Letters 69 (1999) 288.
6. H.H. He *et al.*, Astrop. Phys. 27 (2007) 528; G. Aielli *et al.* (ARGO-YBJ Collaboration), Astrop. Phys. 30 (2009) 287.